CHEMBIOCHEM

DOI: 10.1002/cbic.200700660

A Novel Sensor Platform Based on Aptamer-Conjugated Polypyrrole Nanotubes for Label-Free Electrochemical Protein Detection

Hyeonseok Yoon,[a] June-Hyung Kim,[b] Nahum Lee,[c] Byung-Gee Kim,[c] and Jyongsik Jang*[a]

We first present a simple yet versatile strategy for the functionalization of polymer nanotubes in a controlled fashion. Carboxylic-acid-functionalized polypyrrole (CPPy) nanotubes were fabricated by using cylindrical micelle templates in a water-in-oil emulsion system, and the functional carboxyl groups were effectively incorporated into the polymer backbone during the polymerization by using pyrrole-3-carboxylic acid (P3CA) as a co-monomer without a sophisticated functionalization process. It was noteworthy that the chemical functionality of CPPy nanotubes was readily controlled in both qualitative and quantitative aspects. On the basis of the controlled functionality of CPPy nanotubes, a field-effect transistor (FET) sensor platform was constructed to detect specific biological entities by using a buffer solution as a liquid-ion gate. The CPPy nanotubes were covalently immobilized onto the microelectrode substrate to make a good electrical contact with the metal electrodes, and thrombin aptamers were bonded to the nanotube surface via covalent linkages as the molecular recognition element. The selective recognition ability of thrombin aptamers combined with the charge transport property of CPPy nanotubes enabled the direct and label-free electrical detection of thrombin proteins. Upon exposure to thrombin, the CPPy nanotube FET sensors showed a decrease in current flow, which was probably attributed to the dipole–dipole or dipole–charge interaction between thrombin proteins and the aptamer-conjugated polymer chains. Importantly, the sensor response was tuned by adjusting the chemical functionality of CPPy nanotubes. The efficacy of CPPy nanotube FET sensors was also demonstrated in human blood serum; this suggests that they may be used for practical diagnosis applications after further optimization.

Introduction

The ability to precisely control the size, shape, and surface functionality of organic/inorganic materials has been continuously required for contemporary developments in the fields of catalysts, batteries, electronic devices, drug delivery systems, and so forth. Recently, nanometer-sized particles with controlled shapes have aroused burgeoning interest because of the beneficial properties that are derived from their high surface area and small dimensions.[1,2] Over the last decade in particular, numerous studies on the synthesis and physical properties of carbon nanotubes (CNTs) have been carried out and, in turn, have opened new avenues for advanced device applications. One notable example is the CNT-based biological sensing system.[3] CNTs were functionalized with biomolecules via covalent or noncovalent couplings and then used to detect complementary bioconjugated molecules.[4,5] For the covalent couplings, functional groups including hydroxyl, carbonyl and carboxyl groups were introduced onto the surface of CNTs through acid or plasma treatment. In the case of noncovalent couplings, CNTs were wrapped with various functional materials such as amphiphilic molecules, polymers, and biomaterials through van der Waals force or π–π stacking. However, these functionalization approaches have to inevitably go through complicated reaction steps, and the physical properties of CNTs might be degraded during the process.[6] Furthermore, it is difficult to control the surface functionality in both qualitative and quantitative aspects, and the functional groups that are generated are often unstable under certain environmental conditions. All other nanomaterials with inert surfaces also suffer from the same issues. Hence, there is still an urgency to develop an efficient route to the surface functionalization of nanomaterials.

Compared with other metals and inorganic semiconductors, conducting polymers have offered new opportunities for potential applications by virtue of their inherent characteristics (e.g., facile synthesis, tunable conductivity, structural diversity/flexibility, and cost effectiveness).[7] In particular, 1D-conducting polymer nanomaterials have emerged as excellent candidates for fabricating state-of-the art sensor devices.[8,9] The 1D geometry of the nanomaterials provides remarkable advantages over their film-type counterparts, such as unique anisotropic electronic properties and simple integration with two-terminal microcircuits.[10,11] More specifically, when used as the conduc-

[a] *H. Yoon, Prof. J. Jang*
Hyperstructured Organic Materials Research Center
School of Chemical and Biological Engineering, Seoul National University
Shinlimdong 56-1, Seoul 151-742 (Korea)
Fax: (+82) 2-888-1604
E-mail: jsjang@plaza.snu.ac.kr

[b] *Prof. J.-H. Kim*
Department of Chemical Engineering, Dong-A University
Hadan2dong 840, Busan 604-714 (Korea)

[c] *N. Lee, Prof. B.-G. Kim*
Institute of Molecular Biology and Genetics
School of Chemical and Biological Engineering, Seoul National University
Shinlimdong 56-1, Seoul 151-742 (Korea)

tive channel of field-effect transistor (FET) sensors, 1D-conducting polymer nanomaterials avoid the loss in signal intensity by lateral current shunting, and can present improved sensitivity through depletion or accumulation of charge carriers in the bulk of the nanoscale materials, not only in the surface region.[12] However, for their practical application to various sensor devices, above all, a reliable approach to large-scale production and precise manipulation of 1D-conducting polymer nanomaterials has to be exploited. In the past,[13,14] we have explored the fabrication of several kinds of 1D nanomaterials by using surfactant templates. It was noteworthy that the soft template approach was straightforward and adaptable to large-scale production.

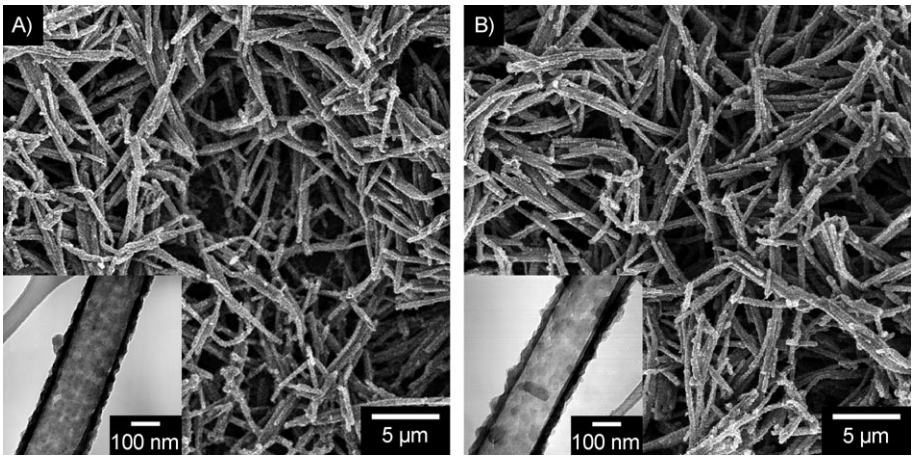

Figure 1. FE-SEM and TEM (inset) images of CPPy nanotubes with different chemical functionalities: A) CPNT-1, B) CPNT-2.

While there has been plenty of information on the demonstration of FET sensors by using CNTs and 1D inorganic semiconductor nanomaterials,[3,11] relatively little research has been done on the application of 1D-conducting polymer nanomaterials to FET sensors, especially biosensors.[12] Herein, we describe a new method for constructing a liquid, ion-gated FET sensor platform that is based on the controlled chemical functionality of conducting polymer nanotubes. Moreover, we also examined its performance for selectively recognizing specific biological species. As a model case, the aptamer–protein interaction was chosen to demonstrate the applicability of the sensor device.

Results and Discussion

First of all, carboxylic-acid-functionalized polypyrrole (CPPy) nanotubes were successfully fabricated by copolymerizing pyrrole-3-carboyxlic acid (P3CA) with pyrrole in a reverse (water-in-oil) microemulsion system. The P3CA functional units were incorporated into the pyrrole repeating units through α–α' covalent linkages without any degradation in their major physical properties. Importantly, the carboxylic acid groups that were introduced can be used as multifunctional sites 1) to covalently bond specific biomolecules to the nanotube surfaces and 2) to immobilize the nanotube bodies onto a substrate. In addition, the chemical functionality of the nanotubes was quantitatively tuned by adjusting the feeding amount of P3CA. Figure 1 shows field emission scanning electron microscopy (FE-SEM) and transmission electron microscopy (TEM) images of CPPy nanotubes with different chemical functionalities. The CPPy nanotubes were fabricated with the P3CA-to-pyrrole molar ratios of 1:15 (CPNT-1) and 1:30 (CPNT-2). The reverse cylindrical micelles that were generated under the same condition served as templates for each P3CA/pyrrole copolymerization. Accordingly, the resulting nanotubes exhibited similar dimensions regardless of their chemical functionality: 30–40 nm in wall-thickness, and 200–250 nm in diameter.

CPPy nanotubes were characterized by X-ray photoelectron spectroscopy (XPS) analysis to inspect their chemical functionality. Figure 2 displays the XPS C1s spectra of CPPy nanotubes

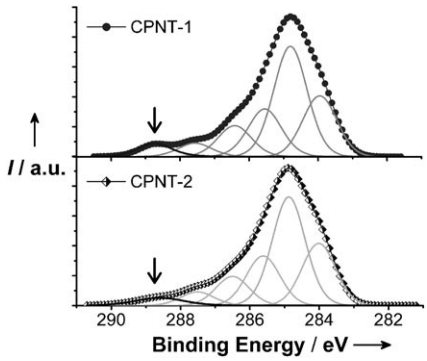

Figure 2. XPS C1s spectra of CPPy nanotubes with different chemical functionalities (the arrow indicates the C1s component that originates from carboxylic acid groups).

with different chemical functionalities. The XPS C1s main peak was deconvoluted into individual components for gaining qualitative information, and the assignment of C1s components is summarized in Table 1. The C1s component that origi-

Table 1. Assignment of XPS C1s components for CPPy nanotubes

No.[a]	Binding energy[b] [eV]	Assignment
C1	288.7	O–C=O
C2	287.6	$C{=}N^+$
C3	286.5	$C{-}N^+$, C≡N
C4–C6	285.6, 284.9, 284.0	C_α[c] C_β[c]

[a] Each component (C) was numbered in the order from high binding energy to low binding energy. [b] Averaged values for both CPNT-1 and CPNT-2. [c] Carbons that exist in two types of pyrrole rings.

nates from the carboxylic acid groups was clearly observed around 288.7 eV (indicated by the arrow). The contribution of the carboxylic acid component was larger in the spectrum of CPNT-1 (atomic ratio $A_{C1}/A_{C\_total} = 0.054$) than in the spectrum of CPNT-2 ($A_{C1}/A_{C\_total} = 0.032$). This result suggests that the controlled amounts of P3CA were successfully incorporated into the polymer chains.

To provide more insight into the chemical functionality, CPPy nanotubes were conjugated with a fluorescent dye that bears a carboxyl moiety, that is, pyreneacetic acid. Figure 3 illustrates the reaction procedure for covalent immobilization of fluorescent dye molecules on the nanotube surface. The first step involves the coupling reaction of CPPy nanotubes with ethylenediamine as a diamino linker; this leads to the amino functionalization of the nanotubes. Covalently linked amine terminal groups act as anchoring sites for carboxyl compounds. In the second step, pyreneacetic acid molecules are covalently bonded to the nanotube surface by a condensation reaction between the carboxyl groups and the surface amino groups. The fluorescence dye molecules were tracked in the samples by using CLSM. As shown in Figure 4, the nanotubes exhibited cyan emission (bright region) with uniform distribution over their surfaces. Judging from these results, the carboxyl groups were thoroughly introduced into the polymer chains, and the availability of the carboxyl groups as multifunctional sites was also confirmed.

The CPPy nanotubes with controlled chemical functionalities can be used as signal transducers for recognizing chemical and biological species. Metal and inorganic semiconductor nanomaterials, including CNTs are commonly integrated with an electrode substrate by photolithography or e-beam lithography. However, conducting polymer nanomaterials could be inadequate for the lithographic process because of possible chemical, thermal, and kinetic damages. In addition, conducting polymers have inherently low adhesion to the electrode substrate.[15] For these reasons, most conducting polymer nanomaterials have been employed for the detection of analytes in the gas phase exclusively, and not in the liquid phase. To overcome this limitation, CPPy nanotubes were chemically tethered onto a surface-modified substrate. The overall reaction steps are represented in Figure 5. Above all, the surface of the microelectrode substrate was modified with primary amino groups by using (3-aminopropyl)trimethoxysilane (APS), and then the nanotubes were immobilized onto the substrate through coupling reactions between the carboxyl groups of CPPy and the amino groups of APS. Subsequently, amine-terminated thrombin aptamers as bioreceptors were selectively bound to the nanotubes through identical coupling reactions without binding to microelectrodes and substrate. For the covalent binding of thrombin aptamers to the carboxyl groups, the 3′-end of the thrombin aptamer (a 15-mer single-stranded DNA aptamer: 5′-GGTTGGTGTGGTTGG-3′) was modified with a primary aliphatic amino linker. In comparison with the attachment of functional biomaterials by physical adsorption, this covalent functionalization offers outstanding stability against environmental perturbation.

Figure 6 displays the FE-SEM image of the nanotubes that are deposited on the interdigitated microelectrodes. The nanotubes formed networks on the electrodes, and provide a sufficient population of the nanotubes for desirable sensor perfor-

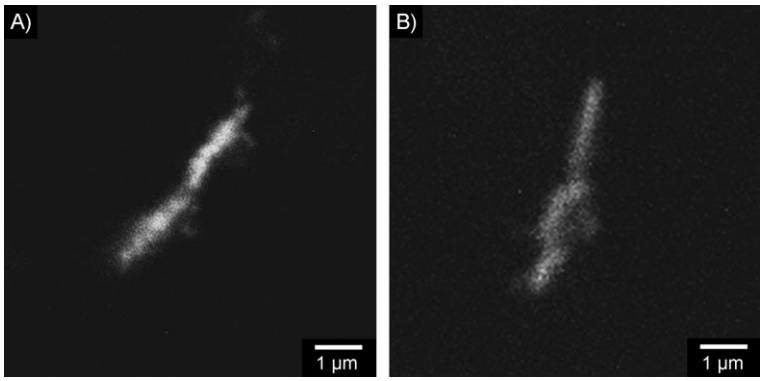

Figure 4. CLSM images of pyreneacetic-acid-conjugated CPPy nanotubes ($\lambda_{exc} = 458$ nm): A) CPNT-1, B) CPNT-2.

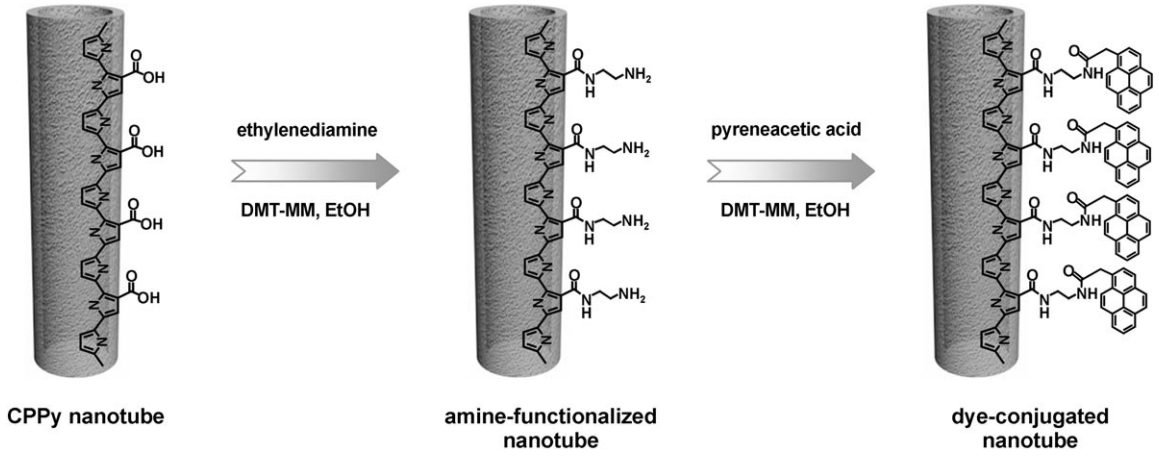

Figure 3. Schematic illustration of reaction steps for the covalent immobilization of fluorescent dye molecules on the surface of CPPy nanotubes.

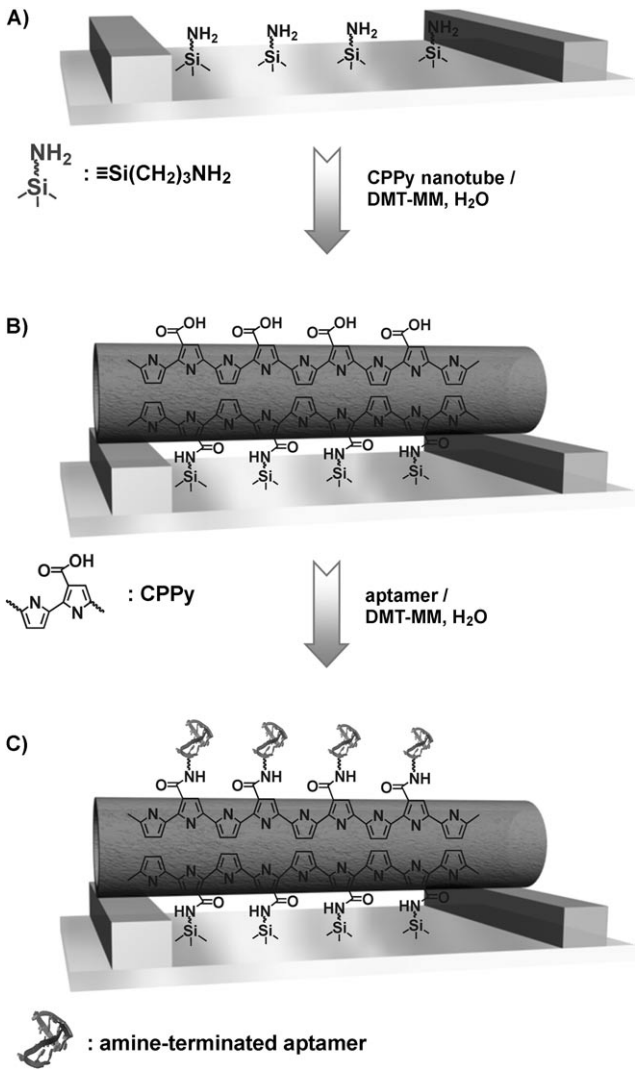

Figure 5. Schematic illustration of reaction steps for the fabrication of sensor platforms based on CPPy nanotubes: A) aminosilane-treated substrate, B) immobilization of the nanotubes onto a substrate, C) binding of biomolecules to the nanotubes.

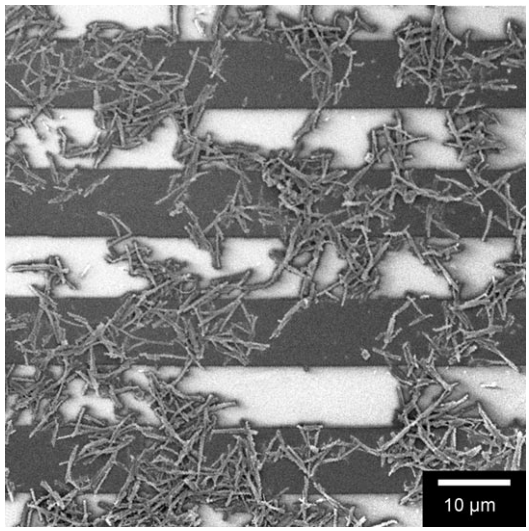

Figure 6. A typical FE-SEM image of CPPy nanotubes that are deposited on the interdigitated microelectrode substrate.

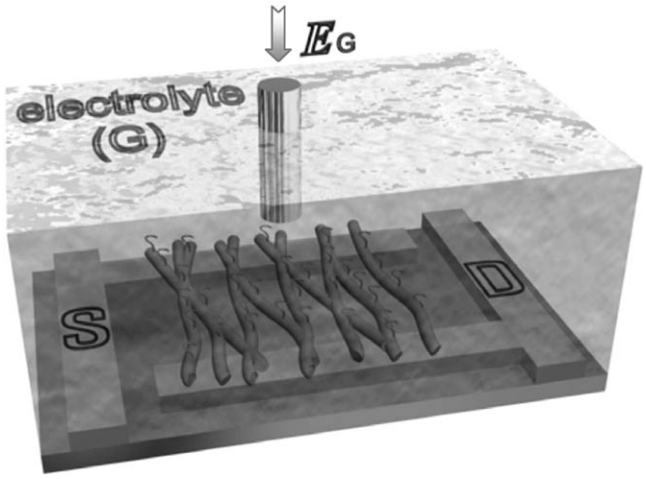

Figure 7. A schematic representation of a CPPy nanotube sensor platform with a FET configuration: the source (S), drain (D), and liquid-ion gate (G) are labelled.

mance. The interdigitated microelectrode configuration allows effective electrical contact between the nanotubes and the electrodes. Therefore, compared with single nanotube devices, the sensor devices that are based on the nanotube networks give more opportunities for specific analytes to come into contact with the nanotubes. From this point of view, the nanotube networks can evoke amplified signals in sensor response, especially at extremely low concentrations.[16,17] In addition, the sensor devices are expected to demonstrate higher reliability in response because the device characteristics such as conductivity and sensitivity are averaged over a large number of the nanotubes.[16,17] Importantly, under our experimental conditions, the CPPy nanotubes that were immobilized onto the substrate were retained without detachment after reaction or washing steps.

To characterize the electrical properties of CPPy nanotubes in liquid phase, a FET configuration was constructed by using an electrolyte as a liquid-ion gate (Figure 7).[18,19] Two Au interdigitated microelectrode bands with 40 fingers (width: 10 μm; length: 4000 μm; interfinger gap: 10 μm) served as source and drain electrodes, respectively. A reference electrode (Ag/AgCl 3 M NaCl) and a counter electrode (Pt wire) were provided in the electrolyte solution for gate control. The gate potential (E_G) was applied between the reference electrode and the nanotubes.

Figure 8 displays the dependence of source–drain current (I_{SD}) versus source–drain voltage (V_{SD}) for varying E_G. Both CPNT-1 and CPNT-2 showed characteristic *p*-type accumulation mode in the E_G range of 0 to −100 mV. Moreover, the I_{SD} that is flowing through the nanotube network channel was modulated by varying E_G. Figure 9 shows the dependence of I_{SD} and transconductance (g_m) on E_G measured at $V_{SD} = -50$ mV. Because polypyrrole is a *p*-type semiconductor in the doped state, the negative E_G can give rise to an increase in the oxida-

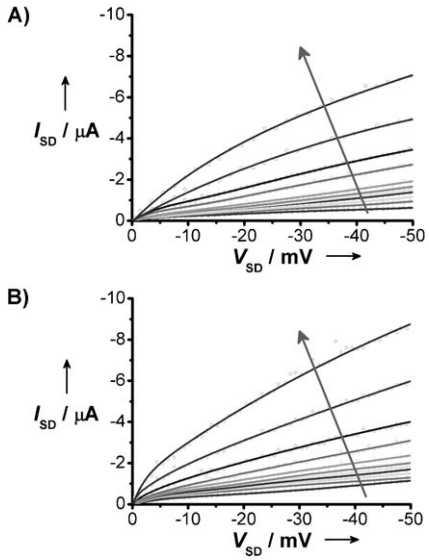

Figure 8. I_{SD}–V_{SD} characteristics of CPPy nanotube FETs for varying E_G from 0 to −100 mV in −10 mV steps: A) CPNT-1, B) CPNT-2.

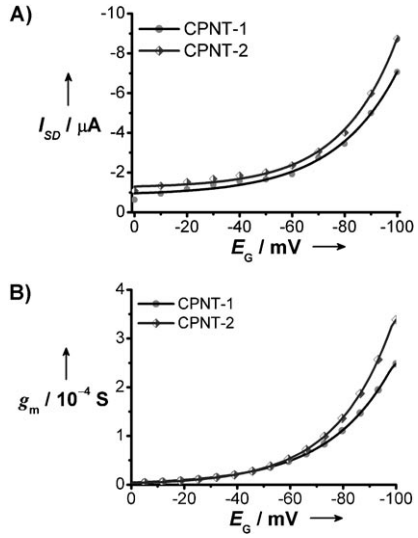

Figure 9. A) I_{SD}–E_G and B) E_G–g_m characteristics of CPPy nanotube FETs for V_{SD} = −50 mV.

tion level of polymer chains. Some potential variations that originate from CPPy–analyte interactions can affect the I_{SD} in a similar manner to the effect of applying E_G. Consequently, the dependence of I_{SD} on E_G confirms that CPPy nanotube FETs can be effectively employed as the electrochemical sensor for detecting analytes in solution. The liquid-ion gating is capable of achieving increased transconductance due to the intimate contact between the nanotubes and the gate compared with conventional back gating.[18,19] The maximum transconductance ($g_{m,\,max}$) values of CPNT-1 and CPNT-2 were 2.5×10^{-4} and 3.4×10^{-4} S, respectively, and these values are approximately 10^2 times higher than those (ca. 10^{-6}–10^{-7} S) of the previously reported polypyrrole FETs.[20,21]

Aptamers, that is, DNA/RNA oligonucleotide probes that can substitute for antibodies and even overcome the drawbacks of antibodies,[22,23] have great potential for biological applications due to their ability to bind target molecules with high affinity and specificity.[24–31] For specific label-free detection of target proteins (human α-thrombin), as described above, the surface of the CPPy nanotubes was covalently functionalized with thrombin aptamers, and was treated with a blocking agent (skim milk) to prevent nonspecific adsorption of undesired species. The sensing test was performed to investigate the dependence of sensor response on the chemical functionality at the V_{SD} (CPNT-1: −15 mV; CPNT-2: −10 mV), where both CPNT-1 and CPNT-2 had similar I_{SD}–E_{GD} characteristics (see Figure 10,

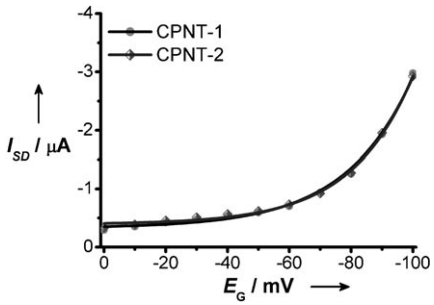

Figure 10. I_{SD}–E_G characteristics for V_{SD} = −15 mV (CPNT-1) and −10 mV (CPNT-2).

$g_{m,\,max}$: ca. 1.2×10^{-4} S). Figure 11 exhibits typical real-time I_{SD} changes (normalized current change, $[\Delta I/I_0]_{SD}$) of FET-type sensors based on aptamer-conjugated CPPy (A-CPPy) nanotubes. The common serum protein, BSA, was employed as a nontarget protein to verify the specificity of A-CPPy nanotubes. Upon addition of BSA, no significant change in I_{SD} was observed: although the signal in the sensor response slightly fluctuated directly after adding the protein solution, it levelled off quickly. When thrombin was added, however, the I_{SD} decreased gradually and reached the saturated value. Namely, it can be considered that the sensor response is highly specific to the binding of thrombin protein to A-CPPy nanotubes.[32–35] The decrease in I_{SD} might account for the intermolecular interaction that is in-

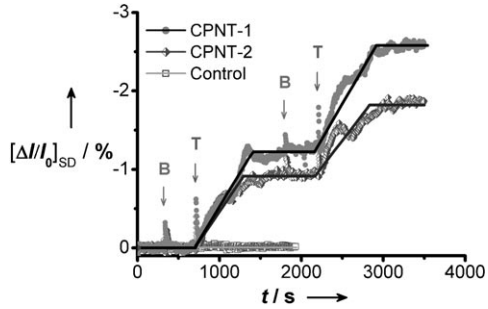

Figure 11. Real-time responses of CPPy nanotube FET sensors measured at V_{SD} = −15 mV (CPNT-1) and −10 mV (CPNT-2): I_{SD} changes upon consecutive additions of 90 nM target (thrombin, T) and nontarget (BSA, B) proteins (the arrow indicates the addition of protein solutions). A control experiment was performed by using CPNT-1 with no thrombin aptamers attached.

duced by the formation of thrombin aptamer–thrombin complex. The P3CA-functionalized unit in the polymer backbone has a large dipole moment ($\mu = 2.06$ D[36]) and the thrombin aptamer has an overall negative charge. Thus, the thrombin that is tethered to A-CPPy nanotubes can lead to dipole–dipole or dipole–charge interactions between thrombin proteins and the aptamer-conjugated polymer chains.[37,38] In particular, the negative charge of the thrombin aptamers can be screened by thrombin proteins when the protein–aptamer complex is formed. Accordingly, this intermolecular interaction could reduce the hopping rate of charge carriers either by increasing the Coulomb interaction between positively charged polymer chains and counterions, or by provoking a conformational change of the polymer chains from a linear conformation into a coil conformation.[37,38] To further confirm that the change in electrical signal was attributed to the specific binding of aptamer to thrombin, a control experiment was carried out by using a FET-type sensor that was based on CPNT-1, with no thrombin aptamers attached. In this case, no measurable change in I_{SD} was detected. As a result, it is evident that A-CPPy nanotubes have the capability to specifically detect the presence of thrombin in solution.

Figure 12 shows the sensitivity changes of A-CPPy nanotubes towards analytes as a function of thrombin concentration. The sensitivity was determined from the absolute value of

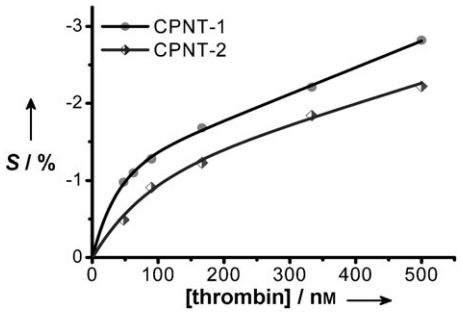

Figure 12. Calibration curves of CPPy nanotube FET sensors that were measured at $V_{SD} = -15$ mV (CPNT-1) and -10 mV (CPNT-2): sensitivity changes as a function of thrombin concentration.

$[\Delta I/I_0]_{SD}$ saturation point, which was measured after the addition of thrombin. The calibration curves presented nonlinear behavior at low concentrations (< 100 nM), but linear behavior was observed over a wide range at high concentrations (ca. 100–500 nM). Importantly, the sensitivity of CPNT-1 was higher than that of CPNT-2 over a wide range of concentration. Considering that CPNT-1 has a higher density of chemical functionality (degree of carboxylic acid group and aptamer introduced) than CPNT-2, the better sensitivity was achieved with CPNT-1 as a result of the enhanced aptamer–protein interaction. The detection-limit concentration of thrombin was approximately 50 nM, which is reasonably comparable to the performance of FET sensors that are based on single-walled CNTs.[39] Several aptamer-based sensor systems that are based on electronic or optical detection have shown detection limits that range from a few nanomolar level to subnanomolar level.[32–35] In general, the response of FET-type sensors is dependent on the conductivity of polymers, interelectrode gap, electrolyte, transconductance, and so forth. Therefore, it is believed that the detection limit might be improved with precise control over the sensor parameters.

In addition, the capability of the sensors to detect specific analytes was examined in a clinically relevant sample, that is, human blood serum. The blood serum has high ionic strength when used without dilution and desalting, this has a strongly negative influence on the sensor response.[40,41] Nevertheless, under our experimental conditions, the sensors exhibited appreciable signals for the undiluted and undesalted human blood serum that contained 166 nM thrombin, as shown in Figure 13. This result suggests the possibility that the CPPy nanotube FET sensors can be used for practical diagnosis applications after further optimization.

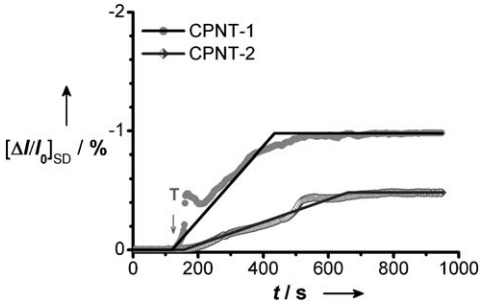

Figure 13. Responses of CPPy nanotube FET sensors measured at $V_{SD} = -15$ mV (CPNT-1) and -10 mV (CPNT-2) in human blood serum: real-time I_{SD} changes upon addition of 166 nM thrombin (the arrow indicates the addition of thrombin, T).

Conclusions

CPPy nanotubes with controlled chemical functionalities were covalently immobilized onto the microelectrode substrate for high-quality electrical contact between polymer transducers and metal electrodes. Consecutively, thrombin aptamers were readily tethered onto the nanotubes by covalent linkages without sophisticated surface treatment. Thus, this fabrication approach might present an efficient route for the construction of sensor platforms that are based on nanoscale polymer transducers that are conjugated with molecular recognition elements. The FET-type sensors that are based on A-CPPy nanotubes were successfully constructed by using liquid-ion gating. The recognition ability of thrombin aptamers, combined with the inherent charge transport property of CPPy nanotubes yielded a direct and label-free electrical readout. Importantly, the sensor response was tunable by adjusting the chemical functionality of the nanotubes; this provides a novel direction for sensitivity control. CPPy nanotubes could be also chemically coupled with fluorescent dyes. Namely, the carboxyl group of the nanotubes allows covalent conjugation with the functional group of various molecules. Accordingly, it is expected

that CPPy nanotubes can be applied to smart transducers[42,43] as well as molecular probes or DNA/protein carriers.[44–46]

Experimental Section

Pyrrole (Aldrich, 98%) and P3CA (Acros Organics, 95%) were used as received. Sodium bis(2-ethylhexyl) sulfosuccinate (AOT; Aldrich, 98%) was employed as a surfactant, and hexane (Aldrich, 99%) was used as an apolar solvent.

CPPy were prepared by copolymerizing pyrrole/P3CA monomers with careful modification of the previous methods. The copolymerization of pyrrole and P3CA proceeded at two different molar ratios to control the chemical functionality. First, AOT (7.9 mmol) was dissolved in hexane (20 mL), and 7 M aq. $FeCl_3$ solution (0.5 mL) was added into the AOT/hexane solution. Subsequently, P3CA was dissolved in pyrrole; the feeding amounts of pyrrole/P3CA were 6 mmol/0.4 mmol and 6 mmol/0.2 mmol for CPNT-1 and CPNT-2 samples, respectively. The pyrrole/P3CA monomers were added stepwise into the AOT/hexane solution, and then the chemical oxidation polymerization proceeded for 2 h at 15 °C. The resulting product was thoroughly washed with excess EtOH to remove the surfactant and other residual reagents. The final product was obtained after drying in a vacuum oven at room temperature. FE-SEM images were taken with a JEOL JSM-6700 F microscope: the samples were coated with a thin layer of gold to eliminate charging effect. TEM images were obtained with a JEOL EM-2000 EXII microscope: the samples were dispersed in an ethanol solution, and were deposited on a carbon mesh foil that was supported on a copper grid. XPS analysis was conducted by using a Thermo VG Scientific Sigma Probe spectrometer with monochromatic $Al_{K\alpha}$ X-ray radiation source.

An efficient condensing agent, 4-(4,6-dimethoxy-1,3,5-triazin-2-yl)-4-methylmorpholinium chloride (DMT-MM), was synthesized according to the procedure described by Kunishima et al.[47] Briefly, 2-chloro-4,6-dimethoxy-1,3,5-triazine was treated with *N*-methylmorpholine/THF (1:1, *v*/*v*) for 30 min. The resulting white precipitates were washed with THF, and then completely dried. The final product was stored in a freezer at under −20 °C. Importantly, DMT-MM was capable of providing excellent yields in the aqueous as well as alcoholic phases for the condensation reaction between carboxylic acid and amine groups.

In order to covalently attach the fluorescent dye to the nanotubes, 0.1 wt% CPPy nanotube EtOH solution (20 μL) was mixed with 10 wt% DMT-MM EtOH solution (20 μL) and ethylenediamine (40 μL) in EtOH (500 μL) for 12 h at 1800 rpm. After washing with distilled water, the nanotubes were mixed with 10 wt% DMT-MM ethanol solution (20 μL) and 5 wt% pyreneacetic acid EtOH solution (40 μL) for 2 h at 1800 rpm. Fluorescence images were obtained with a Carl Zeiss LSM510 confocal laser scanning microscope (CLSM) at the excitation wavelength of 458 nm.

A microarray that consisted of a pair of Au interdigitated microelectrodes with 40 fingers was patterned on a glass substrate by a photolithographic process. The microelectrode substrate was treated with 5 wt% aq. APS solution for 6 h and then exposed to the mixture of 0.1 wt% CPPy nanotube EtOH solution (10 μL) and 10 wt% DMT-MM EtOH solution (10 μL) for 12 h. The resulting CPPy nanotube-immobilized substrate was rinsed with distilled water. Consecutively, the coupling reaction to attach aptamers on the nanotube surface was carried out by using the mixture of 10 wt% aq. DMT-MM solution (10 μL), and 1 μM amine-terminated thrombin aptamer (2 μL) for 12 h. Afterwards, the substrate was rinsed with distilled water and dried with a stream of nitrogen gas. All electrical measurements were conducted in a buffer solution (20 mM Tri-acetate, 140 mM NaCl, 5 mM KCl, 1 mM $CaCl_2$, 1 mM $MgCl_2$; pH 7.4) with a Keithley 2400 SourceMeter and a Wonatech WBCS 3000 potentiostat. A solution chamber was designed and used for all solution-based measurements. Human α-thrombin and thrombin aptamer were purchased from Sigma–Aldrich and Bioneer Co. (Daejeon, Korea), respectively. Thrombin aptamer was modified at 3′ terminus with a primary aliphatic amino linker, NH_2-$(CH_2)_5CONHCH(CH_2OH)[CH_2OPO(OCH_3)CH_3]$ (length: ca. 1.2 nm). Skim milk was employed as a blocking agent to resist the nonspecific binding. The sensor substrate was treated with 0.1 wt% skim milk solution. Control experiments were performed to test the specificity of the sensor response by using bovine serum albumin (BSA) and pristine CPPy nanotubes: several research groups have been demonstrated the specificity of thrombin aptamers by control experiments by using a non-target protein (IgE)[33] and non-binding sequence aptamers.[34,35] Human blood serum was purchased from Sigma–Aldrich Co. and was used without any dilution or desalting.

Acknowledgements

This work was supported by the Center for Advanced Materials Processing under the 21C Frontier Programs of the Ministry of Commerce, Industry and Energy (MOCIE) and by the Fundamental R&D Program for Core Technology of Materials of the MOCIE.

Keywords: aptamers · biosensors · field-effect transistors · nanotubes · polypyrrole

[1] J. Wang, *Small* **2005**, *1*, 1036–1043.
[2] J. J. Gooding, *Small* **2006**, *2*, 313–315.
[3] B. L. Allen, P. D. Kichambare, A. Star, *Adv. Mater.* **2007**, *19*, 1439–1451.
[4] E. Katz, I. Willner, *ChemPhysChem* **2004**, *5*, 1084–1104.
[5] K. Balasubramanian, M. Burghard, *Small* **2005**, *1*, 180–192.
[6] D. Tasis, N. Tagmatarchis, A. Bianco, M. Prato, *Chem. Rev.* **2006**, *106*, 1105–1136.
[7] J. Jang, *Adv. Polym. Sci.* **2006**, *199*, 189–259.
[8] R. A. Potyrailo, *Angew. Chem.* **2006**, *118*, 718–738; *Angew. Chem. Int. Ed.* **2006**, *45*, 702–723.
[9] G. G. Wallace, L. A. P. Kane-Maguire, *Adv. Mater.* **2002**, *14*, 953–960.
[10] a) H. Yoon, M. Chang, J. Jang, *J. Phys. Chem. B* **2006**, *110*, 14074–14077; b) J. Jang, M. Chang, H. Yoon, *Adv. Mater.* **2005**, *17*, 1616–1620.
[11] F. Patolsky, G. Zheng, C. M. Lieber, *Anal. Chem.* **2006**, *78*, 4261–4269.
[12] A. K. Wanekaya, W. Chen, N. V. Myung, A. Mulchandani, *Electroanalysis* **2006**, *18*, 533–550.
[13] a) J. Jang, J. Bae, *Angew. Chem.* **2004**, *116*, 3891–3894; *Angew. Chem. Int. Ed.* **2004**, *43*, 3803–3806; b) J. Jang, H. Yoon, *Adv. Mater.* **2004**, *16*, 799–802; c) J. Jang, H. Yoon, *Adv. Mater.* **2003**, *15*, 2088–2091; d) H. Yoon, J. Y. Hong, J. Jang, *Small* **2007**, *3*, 1774–1783.
[14] a) J. Jang, H. Yoon, *Langmuir* **2005**, *21*, 11484–11489; b) H. Yoon, M. Chang, J. Jang, *Adv. Funct. Mater.* **2007**, *17*, 431–436.
[15] B. Dong, M. Krutschke, X. Zhang, L. Chi, H. Fuchs, *Small* **2005**, *1*, 520–524.
[16] D. Zhang, Z. Liu, C. Li, T. Tang, X. Liu, S. Han, B. Lei, C. Zhou, *Nano Lett.* **2004**, *4*, 1919–1924.
[17] M. Curreli, C. Li, Y. Sun, B. Lei, M. A. Gundersen, M. E. Thompson, C. Zhou, *J. Am. Chem. Soc.* **2005**, *127*, 6922–6923.
[18] M. Krüger, M. R. Buitelaar, T. Nussbaumer, C. Schönenberger, L. Forró, *Appl. Phys. Lett.* **2001**, *78*, 1291–1293.
[19] K. Besteman, J.-O. Lee, F. G. M. Wiertz, H. A. Heering, C. Dekker, *Nano Lett.* **2003**, *3*, 727–730.
[20] C. C. Bof Bufon, T. Heinzel, *Appl. Phys. Lett.* **2006**, *89*, 012104.

[21] M. S. Lee, H. S. Kang, H. S. Kang, J. Joo, A. J. Epstein, J. Y. Lee, *Thin Solid Films* **2005**, *477*, 169–173.
[22] M. Rimmele, *ChemBioChem* **2003**, *4*, 963–971.
[23] S. Jhaveri, M. Rajendran, A. D. Ellington, *Nat. Biotechnol.* **2000**, *18*, 1293–1297.
[24] J. Liu, Y. Lu, *Angew. Chem.* **2006**, *118*, 96–100; *Angew. Chem. Int. Ed.* **2006**, *45*, 90–94.
[25] W. Zhao, W. Chiuman, M. A. Brook, Y. Li, *ChemBioChem* **2007**, *8*, 727–731.
[26] M. V. Yigit, D. Mazumdar, H. K. Kim, J. H. Lee, B. Odintsov, Y. Lu, *ChemBioChem* **2007**, *8*, 1675–1678.
[27] M. Zayats, Y. Huang, R. Gill, C. a. Ma, I. Willner, *J. Am. Chem. Soc.* **2006**, *128*, 13666–13667.
[28] B. R. Baker, R. Y. Lai, M. S. Wood, E. H. Doctor, A. J. Heeger, K. W. Plaxco, *J. Am. Chem. Soc.* **2006**, *128*, 3138–3139.
[29] H. Zhang, Z. Wang, X. F. Li, X. Chris Le, *Angew. Chem.* **2006**, *118*, 1606–1610 ; *Angew. Chem. Int. Ed.* **2006**, *45*, 1576–1580.
[30] M. Levy, S. F. Cater, A. D. Ellington, *ChemBioChem* **2005**, *6*, 2163–2166.
[31] N. Rupcich, R. Nutiu, Y. Li, J. D. Brennan, *Angew. Chem.* **2006**, *118*, 3373–3377; *Angew. Chem. Int. Ed.* **2006**, *45*, 3295–3299.
[32] Y. Xiao, B. D. Piorek, K. W. Plaxco, A. J. Heeger, *J. Am. Chem. Soc.* **2005**, *127*, 17990–17991.
[33] C. Lin, E. Katilius, Y. Liu, J. Zhang, H. Yan, *Angew. Chem.* **2006**, *118*, 5422–5427; *Angew. Chem. Int. Ed.* **2006**, *45*, 5296–5301.
[34] M. B. Abérem, A. Najari, H. A. Ho, J. F. Gravel, P. Nobert, D. Boudreau, M. Leclerc, *Adv. Mater.* **2006**, *18*, 2703–2707.
[35] H.-A. Ho, M. Leclerc, *J. Am. Chem. Soc.* **2004**, *126*, 1384–1387.
[36] The dipole moment was calculated by using the CS Chem3D Pro®.
[37] J. Ouyang, C. W. Chu, F. C. Chen, Q. Xu, Y. Yang, *Adv. Funct. Mater.* **2005**, *15*, 203–208.
[38] J. Y. Kim, J. H. Jung, D. E. Lee, J. Joo, *Synth. Met.* **2002**, *126*, 311–316.
[39] H.–M. So, K. Won, Y. H. Kim, B. K. Kim, B. H. Ryu, P. S. Na, H. Kim, J. O. Lee, *J. Am. Chem. Soc.* **2005**, *127*, 11906–11907.
[40] J. Liu, D. Mazumdar, Y. Lu, *Angew. Chem.* **2006**, *118*, 8123–8127; *Angew. Chem. Int. Ed.* **2006**, *45*, 7955–7959.
[41] Y. Xiao, A. A. Lubin, A. J. Heeger, K. W. Plaxco, *Angew. Chem.* **2005**, *117*, 5592–5595; *Angew. Chem. Int. Ed.* **2005**, *44*, 5456–5459.
[42] N. H. Elowe, R. Nutiu, A. Allali-Hassani, J. D. Cechetto, D. W. Hughes, Y. Li, E. D. Brown, *Angew. Chem.* **2006**, *118*, 5776–5780; *Angew. Chem. Int. Ed.* **2006**, *45*, 5648–5652.
[43] L. L. Kiessling, J. E. Gestwicki, L. E. Strong, *Angew. Chem.* **2006**, *118*, 2408–2429; *Angew. Chem. Int. Ed.* **2006**, *45*, 2348–2368.
[44] R. Chhabra, J. Sharma, Y. Ke, Y. Liu, S. Rinker, S. Lindsay, H. Yan, *J. Am. Chem. Soc.* **2007**, *129*, 10304–10305.
[45] M. Awais, M. Sato, X. Lee, Y. Umezawa, *Angew. Chem.* **2006**, *118*, 2773–2778; *Angew. Chem. Int. Ed.* **2006**, *45*, 2707–2712.
[46] Y. V. Bagalkot, O. C. Farokhzad, R. Langer, S. Jon, *Angew. Chem.* **2006**, *118*, 8329–8332; *Angew. Chem. Int. Ed.* **2006**, *45*, 8149–8152.
[47] M. Kunishima, C. Kawachi, K. Hioki, K. Terao, S. Tani, *Tetrahedron* **2001**, *57*, 1551–1558.

Received: November 3, 2007
Published online on February 5, 2008

